

Resynchronization of the Asynchronous Polar CD Ind

Gordon Myers

CBA (San Mateo) and AAVSO, 5 Inverness Way, Hillsborough, CA 94010, USA;
gordonmyers@hotmail.com

Joseph Patterson

Department of Astronomy, Columbia University, 550 West 120th Street, New York, NY 10027, USA;
jop@astro.columbia.edu

Enrique de Miguel

CBA (Huelva), Observatorio Astronomico del CIECEM, Parque Dunar Matalascañas, 21760 Almonte, Huelva, Spain;
Departamento de Ciencias Integradas, Facultad de Ciencias Experimentales, Universidad de Huelva, 21071 Huelva, Spain; edmiguel63@gmail.com

Franz-Josef Hamsch

CBA (Mol), Oude Bleken 12, B-2400 Mol, Belgium; hamsch@telenet.be

Berto Monard

CBA (Pretoria), PO Box 281, Calitzdorp 6660, Western Cape, South Africa; bmonard@mweb.co.za

Greg Bolt

CBA (Perth), 295 Camberwarra Drive, Craigie, Western Australia 6025, Australia; gbolt@inet.net.au

Jennie McCormick

CBA (Pakuranga), Farm Cove Observatory, 2/24 Rapallo Place, Farm Cove, Auckland, New Zealand, 2012; farmcoveobs@xtra.co.nz

Robert Rea

CBA (Nelson), Regent Lane Observatory, 8 Regent Lane, Richmond, Nelson 7020, New Zealand;
reamarsh@ihug.co.nz

William Allen

CBA (Blenheim), Vintage Lane Observatory, 83 Vintage Lane, RD 3, Blenheim 7273, New Zealand;
whallen@xtra.co.nz

Abstract

CD Ind is one of only four confirmed asynchronous polars (APs). APs are strongly magnetic cataclysmic variables of the AM Herculis subclass with the characteristic that their white dwarfs rotate a few per cent out of synchronism with their binary orbit. Theory suggests that nova eruptions disrupt previously synchronized states. Following the eruption, the system is expected to rapidly resynchronize over a timescale of centuries. The other three asynchronous polars - V1432 Aql, BY Cam and V1500 Cyg - have resynchronization time estimates ranging from 100 to more than 3500 years, with all but one being less than 1200 years. We report on the analysis of over 46000 observations of CD Ind taken between 2007 and 2016, combined with previous observations from 1996, and estimate a CD Ind resynchronization time of 6400 ± 800 years. We also estimate an orbital period of 110.820(1) minutes and a current (2016.4) white dwarf spin period of 109.6564(1) minutes.

Keywords: novae, cataclysmic variables, stars: individual (CD Ind, V1432 Aql, BY Cam, V1500 Cyg),

1 Introduction

CD Ind was discovered during the EUVE all-sky survey (EUVE 2115-58.6: Bowyer et al. 1996) and the ROSAT all sky survey (RX J2115-5840: Voges et al. 1996). Optical spectra (Craig, 1996), spectroscopic observations (Vennes et al. 1996) and optical polarimetry (Schwope et al. 1997) confirmed CD Ind to be a member of the polar subclass of magnetic cataclysmic variables.

In polars the white dwarf's strong magnetic fields (typically > 10 MG) preclude the formation of an accretion disk. Instead, matter from the secondary star flows directly along the magnetic field lines onto one or both of the white dwarf's magnetic poles. The strength of the magnetic fields of polars typically synchronizes the spin of the white dwarf with the orbital period of the binary system.

But asynchronous polars (APs) – a small subset of the polars – exhibit orbital periods near but not equal to the white dwarf spin. Optical polarimetry observations (Ramsay et al., 1999) confirmed CD Ind as a member of this rare subclass. CD Ind has a 1.2 per cent difference between the white dwarf spin and binary orbital period.

Currently there are four confirmed asynchronous polars – V1432 Aql, BY Cam, V1500 Cyg and CD Ind.¹

¹ A fifth star, 1RXS J052430.2+424449 (“Paloma”) is sometimes shown as a fifth member of the AP class. While it shows the two-period behavior that is the main credential for the class (Schwarz et al. 2007), its light curve shows many additional periodic signals and its proper classification is still uncertain.

The cause of their asynchronous behavior is theorized to be an eruption on the surface of the white dwarf disrupting a previously synchronized state. V1500 Cyg was the first detected AP showing the asynchronous condition following its 1975 nova eruption. The three other stars plausibly fit this scenario, but are more speculative since the nova event blamed for the asynchronism is only hypothesized, not actually observed. A recent attempt to estimate eruption dates of APs by searching for their nova shell remnants resulted in no shell detections (Pagnotta et al., 2016).

Following the nova disruptive event, it is theorized that resynchronization between the white dwarf and orbital period occurs rapidly (on the order of centuries).² Table 1 shows current estimates for V1432 Aql, BY Cam, and V1500 Cyg resynchronization times (t_{sync}). The objective for this study is to determine CD Ind’s resynchronization time and compare it to the other three asynchronous polars.

Table 1 – The Asynchronous Polars

System	P_{orb} (h)	P_{spin} (h)	$(P_{\text{orb}} - P_{\text{spin}}) / P_{\text{orb}}$	t_{sync} in years [source]
V1432 Aql	3.3655 [1]	3.3751 [2]	-0.0029	110[1]; 199[3]; 96.7 [4]
BY Cam	3.3544 [1]	3.3222 [2]	0.0096	1200[5]; 1107[1]; ≥ 3500 [6]; 250[7]
V1500 Cyg	3.3507 [1]	3.2917 [2]	0.0176	185[5]; 150[1]; 150-290 [7]; 39[9]; 170[10]
CD Ind	1.8467 [1]	1.8258 [2]	0.0113	6400 [8]

References: Pagnotta & Zurek (2016); [1] Campbell & Schwope (1999); [2] Ramsay et al. (1999); [3] Staubert et al. (2003); [4] Andronov & Baklanov (2007); [5] Piirola et al. (1994); [6] Honeycutt & Kafka (2005); [7] Pavlenko et al. (2013); [8] this paper; [9] Harrison & Campbell (2016); [10] Schmidt et. al (1995); [10] Schmidt et. al. (1995)

2 Observations

More than 46000 photometric observations taken over 1224 hours on 285 nights were submitted to the Center for Backyard Astrophysics (CBA) (www.cbastro.org) by eight observers between 2007 and 2016. Table 2 shows the spread of observations across those 10 years.

Table 2. Summary of Observations

Year	No. of Runs	No. of Observations	Duration of Observing Sessions (h)	Approximate Number of Spin Cycles Observed
2007	31	8631	153	83

² This point is disputed by Harrison & Campbell (2016) who interpreted their 2014 observations to indicate V1500 Cyg has already synchronized – a mere 39 years after the nova. This point is important since V1500 Cyg is the only AP for which we know the actual date of the nova event. But CBA’s extensive photometry in 2014 shows an obvious detection of the spin period, free from aliases and shorter than P_{orb} by 175 ± 1 s. This is consistent with the other photometrically derived timescales for synchronization in Table 1, as well as the timescale of 170 yr derived by Schmidt et. al. (1995) from polarimetry. These CBA observations will be written up separately.

2008	20	10273	103	56
2011	53	13467	270	148
2013	9	879	27	14
2014	52	1923	163	89
2015	76	7144	295	161
2016	44	3771	213	116
Totals	285	46088	1224	667

The CBA is a global network of small telescopes dedicated to photometry of cataclysmic variables. The observations were taken with telescopes located in South Africa, Chile, Australia and New Zealand. This provides a good longitudinal spread significantly reducing aliases. Table 3 describes the telescopes used by the CBA observers.

Table 3. CBA telescopes used to observe CD Ind from 2007 to 2016.

Observer	Observatory Location	Telescope	CCD	Number of Measured Maxima
Hamsch	San Pedro de Atacama, Chile	Orion Optics ODK 400 mm	FLI w/Kodak 16803	64
Myers	Coonabarabran, Australia	Planewave CDK 410 mm	FLI PL4710	48
Rea	Nelson, New Zealand	2007/2008 - Celestron C11	SBIG ST-402	5
		2007/2008 - Celestron C14	SBIG ST-9	15
		2011 - CDK20	SBIG ST-9	5
McCormick	Auckland, New Zealand	Meade LX200R - 360 mm	SBIG ST-8XME	3
Monard	Pretoria, South Africa	2007/2008-Meade RCX400 - 300 mm	SBIG ST-7XME	18
	Calitzdorp, South Africa	2010- Meade RCX400-350 mm	SBIG ST-8XME	3
Bolt	Perth, Australia	Meade LX200 - 254 mm	SBIG ST-7	3
Allen	Blenheim, New Zealand	Classical Cassegrain - 400 mm	SBIG STL-1001E	1

Observations of CD Ind used exposure times between 30 and 120 sec and either no filter or Clear filters with a UV cutoff. All images were dark subtracted and flat fielded. Timings were adjusted to HJD and observations from different observers were adjusted to yield a common instrumental magnitude, with effective wavelength near 6000 Å (“pink”). Observers used differential photometry using AAVSO and UCAC4 comp magnitudes. Overlap of observing runs between observers were used to develop constants for adjusting the magnitudes to a common baseline.

3 Results

3.1 White Dwarf Spin

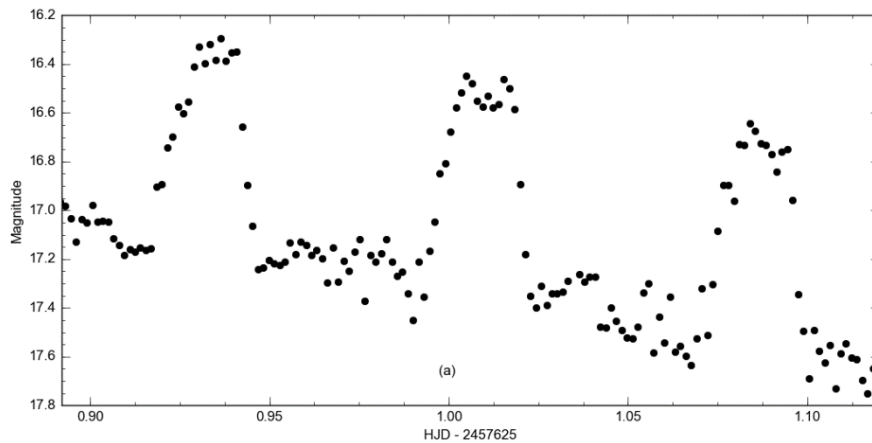
3.1.1 Analysis based on CBA 2007-2016 Observations

Obtaining an accurate value of the spin period requires careful timing of a specific feature observed in each spin cycle. But the hump profiles in CD Ind vary considerably - often changing from night to night, and complicating the task of choosing a consistent marker.

In a fully synchronized polar the accretion flow from the secondary follows a ballistic trajectory until captured by the magnetic field of the primary where it is directed above or below the orbital plane onto the surface of the white dwarf (WD). The relative position of the two stars remains fixed because the WD spin and binary orbit period are locked. A more complex flow is expected to occur in APs since the accretion region on the surface of the white dwarf is not fixed, but changes periodically on the beat cycle (approximately 7.3 days for CD Ind as discussed and calculated in section 3.3).

Like nearly all magnetic CV's, CD Ind sometimes dives into states of very low accretion. The exact cause is not known. This was observed twice during our observations (HJD 2455830.4 and 2457225.2).

The variation in the profile makes it difficult to obtain precise timing measurements of a consistent feature in each cycle. Figure 1 shows three examples of the changing profile probably caused by the ever-changing angle between the two magnetic fields (the white dwarf and the secondary).



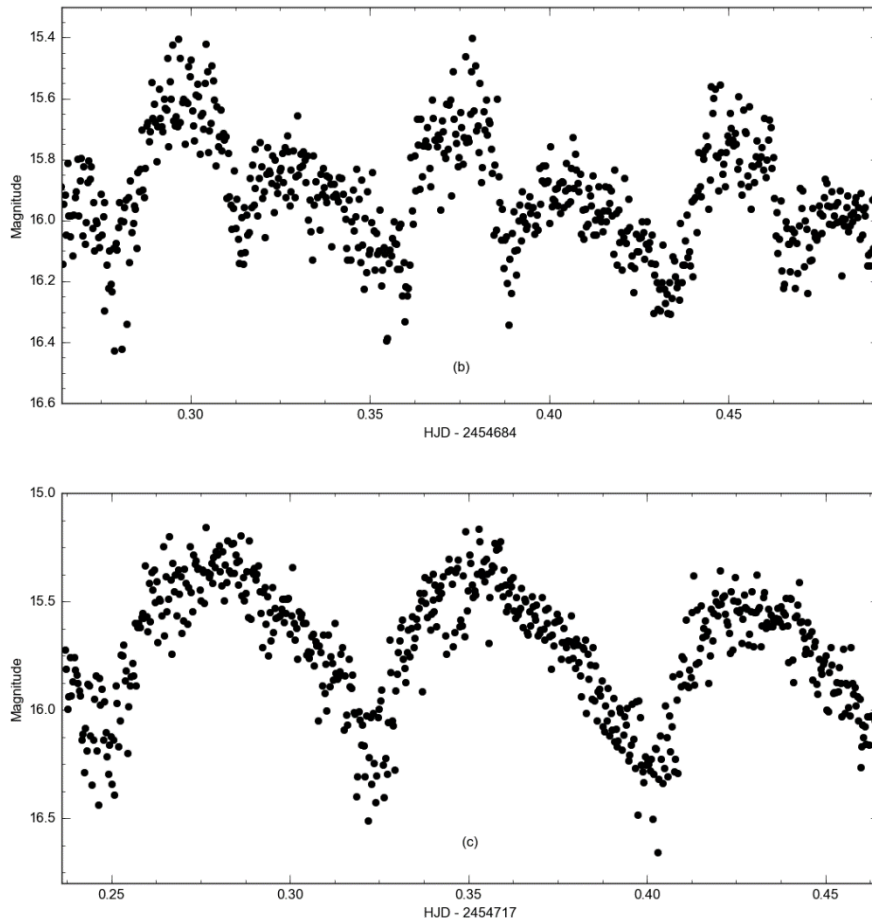


Figure 1 Several nightly light curves of CD Ind, illustrating the variety. We interpret type (a) as signifying accretion onto one magnetic pole, and type (b) as possibly signifying two pole accretion. Type (c) probably arises from one main pole accreting with a changing perspective angle during the white dwarf spin cycle. With this variety we choose only to use type (a) for our period study.

In order to improve the accuracy of the timing of individual maxima, only cycles with light curves clearly showing a profile similar to Figure 1(a) were used. Of the approximate 667 spin cycles observed, 165 had this distinctive profile. Even with these light curves there was no clear marker for precise timings. Many humps exhibit virtually flat profiles near their peak. Therefore, times of maximum light were determined by fitting a quadratic curve to the observed humps and recording the time of maximum light. Figure 2 shows the quadratic fits to three of the peaks observed using different scopes which used different image exposure times.

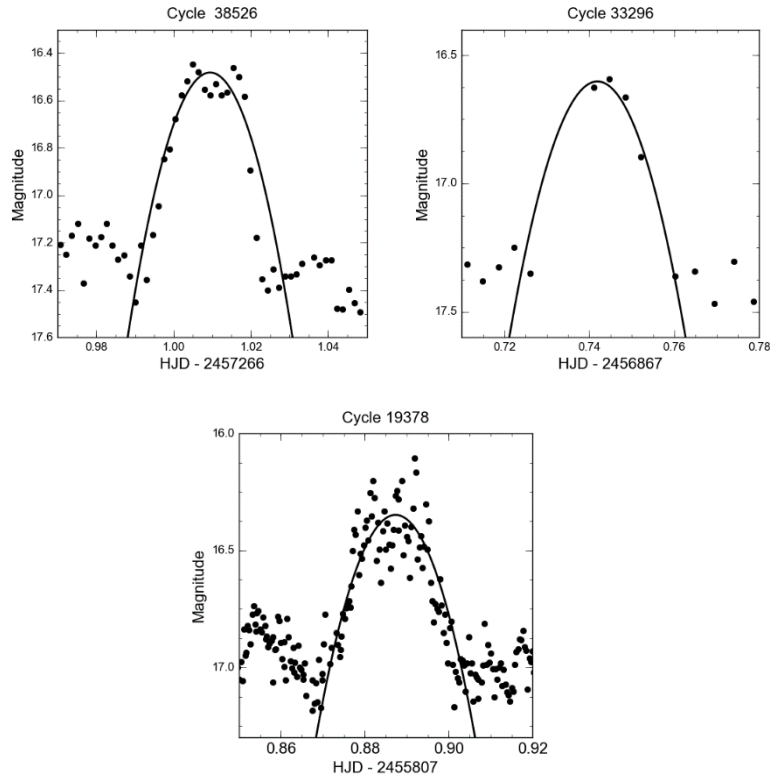


Figure 2. For all profiles of type (a) we determine the time of maximum light by fitting a quadratic. The three plots show different image exposure times used by different observers – 60, 120 and 30 seconds.

After we measured the timings on the 165 selected humps we generated ephemerides using linear and quadratic regressions on the times of maximum light as a function of associated cycle counts.

The linear regression of the measured times of maximum light vs. cycle count yields the following ephemeris with an O-C standard deviation of .0038 d:

$$\text{HJD of mid-humps} = 2454332.2616(38) + 0.07614973(9) E \quad (1)$$

where E is the cycle number. The O-C residuals using equation (1) are shown in Figure 3. A quadratic regression to these residuals yields the curve shown indicating a changing white dwarf spin period.

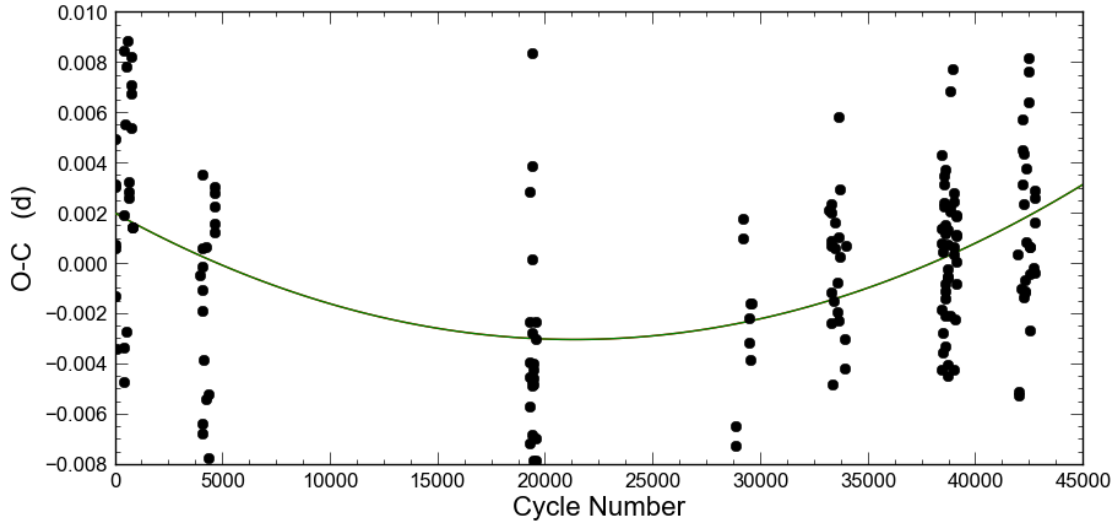


Figure 3. O-C diagram of mid-hump times, relative to a test period of 0.07614973 days (equation (1)). The quadratic fit yields $dP_{\text{spin}}/dt = 2.9(4) \times 10^{-10}$

The quadratic regression of the measured times of maximum light vs. cycle count yields the following ephemeris with an O-C standard deviation of 0.0034 d :

$$\text{HJD of mid-humps} = 2454332.2637(34) + 0.07614926(8) E + 1.10(18) \times 10^{-11} E^2 \quad (2)$$

3.1.2 Incorporation of Schwope et al. data from 1996

In addition to the 165 timings measured using the CBA data, four timings of mid-hump peaks observed in 1996 were available from Schwope et al. (1997). Because of uncertainty about exactly how the measurements were made – and the fact there is an 11-year gap with the CBA data, analysis was first performed on only the CBA data. Then the effect of including Schwope’s additional four earlier measurements was evaluated.

Schwope et al. 1997 contains four mid-hump timings “...derived for far-pole accretion” so it appears measurements were made on light curve profiles similar to those used in analyzing CBA data.

A quadratic regression to the combined data yields the following ephemeris with an O-C standard deviation of 0.0034 d:

$$\text{HJD of mid-humps} = 2454332.2641(34) + 0.07614917(8) E + 1.32(18) \times 10^{-11} E^2 \quad (3)$$

The O-C residuals incorporating the Schwöpe data are shown in Figure 4. From the second-order coefficient in equation (3) we infer a value of $dP_{\text{spin}}/dt = 3.5(4) \times 10^{-10}$. Because of the consistency of the results when incorporating the Schwöpe data and the fact that with these data we have a 20-year observation baseline, equation (3) is adopted as the best ephemeris. Based on this ephemeris the white dwarf spin period increases from 109.6528(1) to 109.6564(1) min across the 20 years of observation. This period is consistent with the lower of the two estimates (109.84 or 109.65 minutes) from Schwöpe et al. (1997) which were based on photometric measurements.

In order to be conservative with our error estimates we used the 42752 cycle count from the CBA data rather than the full 95251 cycles starting with Schwöpe’s 1996 observations.

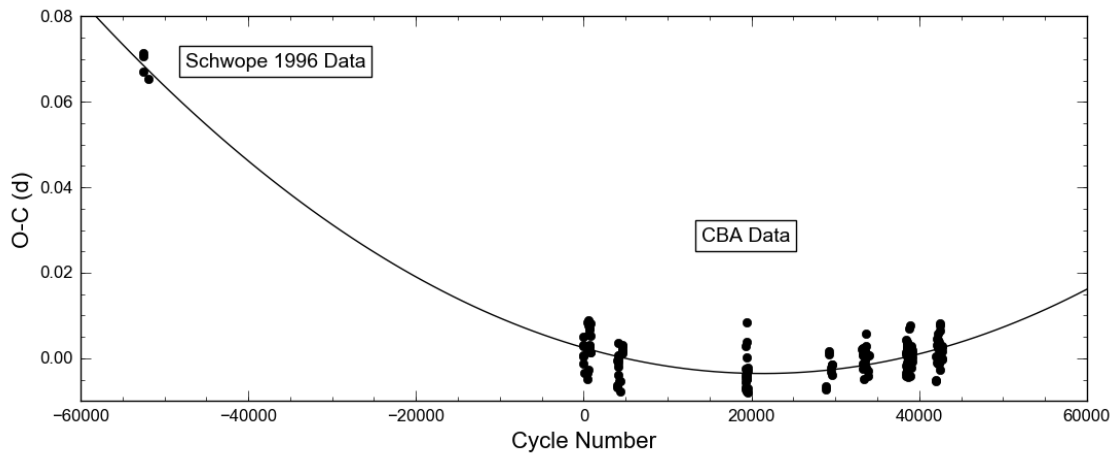


Figure 4. O-C diagram of mid-hump times relative to a test period of 0.07614973 days. The quadratic fit yields $dP_{\text{spin}}/dt = 3.5(4) \times 10^{-10}$

3.2 Orbital Period

We analyzed all the CBA data using the Period04 package (Lenz and Breger, 2005) based on the discrete Fourier transform method. Based on existing information we limited the period search to the interval 12.5 to 13.5 cycles/d to include both the orbital and spin periods. We show the corresponding power spectrum in Figure 6. The spectrum is dominated by a peak centered at 13.1320(14) cycles/d, a value fully consistent with our previous estimate of the spin period.

A peak at a frequency of 12.994939(5) cycles/d, or a periodicity of 110.82005(4) min, is also apparent in the spectrum. This is similar to previous reports of the orbital period of 110.889 minutes from Ramsay et al. (1999) based on polarimetry data and 110.75(6) minutes from Vennes et al. (1996) based on spectroscopy data. Thus we interpret this detection as a footprint of the orbital motion. The error estimates were obtained using Period04’s Monte Carlo simulation.

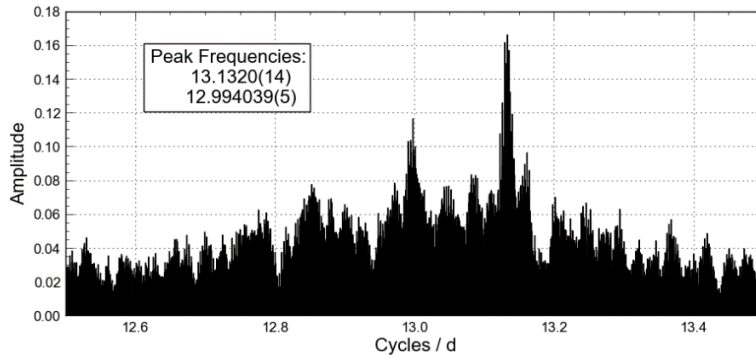


Figure 5. Power Spectrum – the two dominant peaks correlate to the orbital period (12.99 c/d) and the white dwarf spin (13.13 c/d)

3.3 Beat Period

Based on the WD 2015 spin frequency (f_{spin}) of 13.1324 c/d and orbital frequency (f_{orbit}) of 12.9949 c/d, the 2015 beat frequency of 0.137 c/d which equates to a period of 7.299 d. Since the beat period represents the time taken by the secondary to orbit the white dwarf in the frame of the rotating white dwarf, a clear beat period profile was expected. For unknown reasons the strength of the appearance of the beat period varies considerably during different years. The observing year with the most runs – 2015 with 76 runs - shows the most distinctive beat period pattern. Figure 6 shows the light curve folded on the beat period of 7.299 d

The beat period assumes the white dwarf spin is prograde (i.e. the beat frequency is $f_{\text{spin}} - f_{\text{orbit}} = 0.137$ c/d). If the motion were retrograde, the beat frequency would be $f_{\text{spin}} + f_{\text{orbit}} = 26.127$ c/d. Spectral signals were detected at both frequencies with the 0.137 c/d signal having a power amplitude of 0.35 compared to a power amplitude of 0.078 for the 26.127 c/d signal. The significantly higher strength of the 0.137 c/d signal supports the assumption of prograde motion – consistent with the current theory of AP formation.

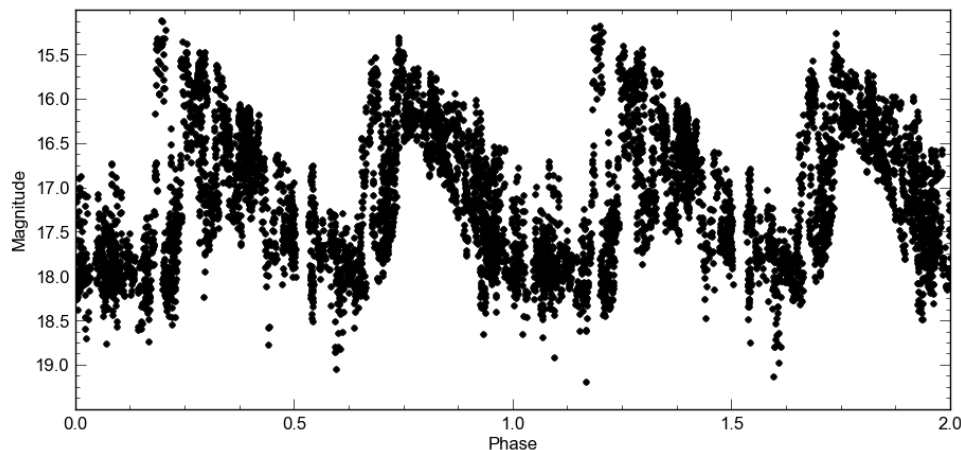


Figure 6. 2015 Folded Light Curve based on a beat period of 7.299 d

4 Conclusion - Resynchronization Projection

A resynchronization time estimate was made by dividing the current difference between the WD spin and orbital spin periods (P_{spin} and P_{orb}) by the white dwarf spin change rate $dP_{\text{spin}}/dt = 3.5(4) \times 10^{-10}$. This assumes the spin change rate is constant over time and yields a resynchronization time of 6400 +/- 800 years.

This predicted resynchronization time is longer than estimates for the other three APs shown in Table 1. The exact reason is not known. One possibility is that the resynchronization rates may not be constant; they may vary over time – e.g. they could decay exponentially as the systems approach synchronism.

Another potential cause relates to the strength of the CD Ind's relatively low magnetic field strength (for a polar). Polars field strength is typically 7 - 230 MG (Ferrario, de Martino & Gänsicke, 2015). Estimates for CD Ind's field are 11 ± 2 MG (Schwope et al. 1992) and < 20 MG (Vennes et al. 1996). Campbell & Schwope (1999) indicate the resynchronization time is inversely proportional to the square of the magnetic field strength. This may be a contributing factor but additional research is required.

Separate from the analysis of the resynchronization time estimate, the question of whether CD Ind's WD spin is prograde or retrograde was examined. The Fourier power spectrum at the two potential interaction frequencies ($f_{\text{spin}} + f_{\text{orb}}$ and $f_{\text{spin}} - f_{\text{orb}}$) was examined. Based on the strength of the signals, CD Ind exhibits prograde motion which is consistent with the current theory of AP evolution.

5 Acknowledgements

We thank the National Science Foundation for support of this research (AST-1211129 and AST-1615456), and NASA through HST-GO-13630. Enrique de Miguel acknowledges financial support from the Ministerio de Educacion, Cultura y Deporte (Spain) under the Mobility Program Salvador de Madariaga (PRX15/00521).

This research made use of Astropy, a community-developed core Python package for Astronomy (Astropy Collaboration, 2013).

6 References

- Andronov I. L., Baklanov A. V., 2007, *Astrophysics*, 50, 105
Bianchini A., Saygac T., Orio M., della Valle M., Williams R., 2012, *A&A*, 539, A94
Bowyer S., Lampton M., Lewis J., Wu X., Jelinsky P., Malina R. F., 1996, *ApJS*, 102, 129
Campbell C. G., Schwope A. D., 1999, *A&A*, 343, 132

Cropper, Mark (1990-12-01). "The polars". *Space Science Reviews* 54 (3-4): 195–295.

Ferrario L., de Martino D., Gänsicke B. T., 2015, *Space Science Rev.*, 191, 111

Harrison T., Campbell R., 2016, *MNRAS*, 459, 4161

Honeycutt R. K., Kafka S., 2005, *MNRAS*, 364, 917

Lenz P., Breger M., 2005, *Commun. Asteroseismol.*, 146, 53

Lipkin Y. M., Leibowitz E. M., 2008, *MNRAS*, 387, 289

Pagnotta A., Zurek D., 2016, *MNRAS*, 458, 1833

Pavlenko E., Andreev M., Babiba Y., Malanushenko V., 2013, in Krzesiński J., Stachowski G., Moskalik P., Bajan K., eds. *ASP Conf. Ser. Vol. 469, 18th European White Dwarf Workshop.*, Astron. Soc. Of the Pac., San Francisco, CA, p.343

Pirola V., Coyne G. V., Takalo S. J., Takalo L., Larsson S., Vilhu O., 1994, *A&A*, 283, 163

Ramsay G., Buckley D., Cropper M., Harrop-Allin M. K., 1999, *MNRAS*, 303, 96

Ramsay G., Potter S., Cropper M., Buckley D., Harrop-Allon M. K., 2000, *MNRAS*, 316, 225

Schmidt G., Liebert J., Stockman H., 1995, *ApJ*, 441, 414

Schwarz R., Schwobe A.D., Staude A., Rau A., Hasinger G., Urrutia T., Motch C., 2007, *A&A*, 473, 511

Schwobe A. D., Buckley D. A. H., O'Donoghue D., Hasinger G., Trümper J., Voges W., 1997, *A&A*, 326, 195

Staubert R., Friedrich S., Pottschmidt K., Benlloch S., Schuh S. L., Knoll P., Splittgerber E., Rothschild R., 2003, *A&A*, 407, 987

Vennes S., Wickramasinghe D., Thorstensen J., Christian D., Bessell M., 1996, *AJ*, 112, 2254

Voges W., et al., 1996,, *IAU Circ.* 6420

Table 4 – Cycle Numbers and HJD Observed Times of mid-humps

Cycle Number	HJD						
-52499	2450334.54400	4638	2454685.44635	33479	2456881.68010	38932	2457296.93072
-52474	2450336.45130	4639	2454685.52325	33492	2456882.66905	38987	2457301.10695
-52473	2450336.52820	4640	2454685.59918	33571	2456888.68350	38998	2457301.94948
-51907	2450379.62310	19270	2455799.66127	33584	2456889.67229	38999	2457302.02535
0	2454332.26465	19272	2455799.81209	33624	2456892.72601	39000	2457302.10395
1	2454332.33648	19283	2455800.65296	33663	2456895.68774	39013	2457303.09357
2	2454332.41465	19284	2455800.73070	33676	2456896.68103	39090	2457308.95241
3	2454332.49067	19285	2455800.80469	33689	2456897.67021	39103	2457309.94566
4	2454332.56936	19298	2455801.80200	33715	2456899.65275	39104	2457310.02258
8	2454332.87578	19376	2455807.73201	33951	2456917.61816	39116	2457310.93370
73	2454337.81716	19377	2455807.81010	33952	2456917.69311	39117	2457311.01075
405	2454363.11072	19378	2455807.88645	33978	2456919.67791	39118	2457311.08874
417	2454364.01799	19380	2455808.04064	38409	2457257.09482	39129	2457311.92560
448	2454366.37335	19388	2455808.65278	38410	2457257.16857	41956	2457527.20009
449	2454366.44815	19391	2455808.88493	38429	2457258.62104	42034	2457533.13419
508	2454370.95123	19392	2455808.96558	38430	2457258.69661	42036	2457533.28663
521	2454371.94349	19462	2455814.27987	38433	2457258.92859	42161	2457542.80942
522	2454372.00906	19467	2455814.66361	38499	2457263.94660	42173	2457543.72877
587	2454376.97035	19468	2455814.74002	38516	2457265.24191	42174	2457543.80353
652	2454381.91409	19473	2455815.12111	38521	2457265.62589	42188	2457544.87224
654	2454382.06614	19474	2455815.19751	38525	2457265.93229	42240	2457548.82865
655	2454382.14292	19556	2455821.43878	38526	2457266.00859	42241	2457548.90110
743	2454388.84762	19558	2455821.59021	38527	2457266.08546	42280	2457551.87661
744	2454388.92414	19571	2455822.58571	38528	2457266.16198	42331	2457555.75478
745	2454389.00139	19573	2455822.73729	38607	2457272.17220	42332	2457555.83088
783	2454391.89223	28889	2456532.14395	38608	2457272.24716	42333	2457555.90754
849	2454396.91419	28890	2456532.22090	38613	2457272.63011	42383	2457559.71656
850	2454396.99031	29230	2456558.12003	38619	2457273.08930	42385	2457559.87177
3965	2454634.19483	29231	2456558.19544	38620	2457273.16579	42464	2457565.89022
4048	2454640.50936	29478	2456577.00024	38621	2457273.24414	42475	2457566.72911
4049	2454640.58510	29498	2456578.52424	38626	2457273.61977	42476	2457566.80579
4059	2454641.35151	29569	2456583.92921	38627	2457273.69649	42517	2457569.91709
4060	2454641.42846	29570	2456584.00761	38697	2457279.02329	42528	2457570.75806
4061	2454641.50556	29583	2456584.99754	38699	2457279.17603	42529	2457570.83311
4062	2454641.58245	33204	2456860.73944	38709	2457279.94133	42530	2457570.91037
4070	2454642.19454	33282	2456866.67463	38710	2457280.01849	42729	2457586.06334
4148	2454648.12686	33295	2456867.66762	38718	2457280.62825	42739	2457586.82663
4241	2454655.20721	33296	2456867.74192	38719	2457280.70256	42740	2457586.90079
4254	2454656.20321	33309	2456868.73538	38725	2457281.15941	42742	2457587.05633
4332	2454662.13706	33321	2456869.64886	38810	2457287.63479	42752	2457587.81755
4333	2454662.21066	33322	2456869.72389	38815	2457288.01137		
4636	2454685.29301	33374	2456873.67794	38827	2457288.92950		
4637	2454685.36950	33400	2456875.66117	38842	2457290.07636		